Modeling the effects of biomass accumulation on the performance of a biotrickling filter packed with PUF support for the alkaline biotreatment of dimethyl disulfide vapors in air.

Luis Arellano-García[a], Antonio D. Dorado[b], Xavier Gamisans[b], Axayacatl Morales-Guadarrama[c, d], Sergio Revah*[e]

[a]Departamento de Ingeniería de Procesos e Hidráulica. UAM Iztapalapa. San Rafael Atlixco 186, Col. Vicentina, Iztapalapa, 09340, México.

[b]Departamento de Ingeniería Minera y Recursos Naturales. UPC. Av. Bases de Manresa 61-73 08242, Manresa-Barcelona.

[c]Departamento de Ingeniería Eléctrica. UAM Iztapalapa. San Rafael Atlixco 186, Col. Vicentina, Iztapalapa, 09340, México

[d]Centro Nacional de Investigación en Imagenología e Instrumentación Médica. UAM Iztapalapa. San Rafael Atlixco 186, Col. Vicentina, Iztapalapa, 09340, México.

[e]Departamento de Procesos y Tecnología. UAM Cuajimalpa. Artificios 40, Col. Hidalgo, Álvaro Obregón, 01120, México.

* srevah@correo.cua.uam.mx. Tel. +52 55 26363801

Abstract

Excess biomass buildup in biotrickling filters leads to low performance. The effect of biomass accumulation in a biotrickling filter (BTF) packed with polyurethane foam (PUF) was assessed in terms of hydrodynamics and void space availability in a system treating dimethyl disulfide (DMDS) vapors with an alkalophilic consortium. A sample of colonized support from a BTF having been operating for over a year was analyzed and it was found that the BTF void bed fraction was reduced to almost half of that calculated initially without biomass. Liquid flow through the examined BTF yielded dispersion coefficient values of 0.30 and 0.72 $m^2\ h^{-1}$, for clean or colonized PUF respectively. 3D images of attached biomass obtained with magnetic resonance imaging allowed to calculate the superficial area, the volume percentage and the biofilm depth as 650 $m^2\ m^{-3}$, 35% and 0.6 mm respectively. A simplified geometric approximation of the complex PUF structure was proposed using an orthogonal 3D mesh which predicted 600 $m^2\ m^{-3}$ for the same biomass content. With this

simplified model it is suggested that the optimum biomass content would be around 20% of bed volume. Biofilm activity was evaluated by respirometry and biological intrinsic kinetics could be described with a Haldane equation type. Experimentally determined parameters were used in a mathematical model to simulate the DMDS elimination capacity (EC) and better description was found when the removal experimental data were matched with a model including liquid axial dispersion in contrast to an ideal plug flow model.

Keywords

Biotrickling filter, MRI, biofilm, modeling, dimethyl disulfide, liquid dispersion

Introduction

Odor control is a priority in populated areas because of public complaints near emission sources or greater environmental awareness reflected in stronger air quality regulation. In this regard, the efficiency of biological processes for the treatment of malodorous sulfur compounds, such as hydrogen sulfide, mercaptans, inorganic and organic sulfides has been thoroughly tested (Smet & Van Langenhove 1998; González-Sánchez et al. 2008; Ramírez et al. 2011; Silva et al. 2012; Estrada et al. 2012).

In biofilters and biotrickling filters, odor causing pollutants in air are transferred to an active biofilm where they are transformed to non-odorous substances while more biomass is produced. Initially, and with adequate environmental conditions including active biomass, sufficient nutrients and well distributed water flow over the packing, biomass growth would be expected to occur by the colonization of all the superficial area of the support. The extended thin layer enhances the contaminant transport to the interior of the biofilm, which remains completely active. Nonetheless, sustained biomass accumulation in BTF packing leads initially to reduced efficiency and ultimately to shut down due different factors. First, at micro and mesoscopic level, the increase in the biofilm depth provokes that the innermost part becomes inactive (by either substrate or oxygen limitation). Secondly, irregularities in liquid and gas flows are developed from biofilm growth leading to fluctuations in the velocity profiles. At macroscopic scale, biomass accumulation induces the narrowing of air and liquid passages with consequent overall residence time reduction and increased pressure drop (Alonso et al. 1996; Trejo-Aguilar et al. 2005; Dorado et al. 2012).

Assessing biomass accumulation in biotrickling filters may be accomplished at both scales by diverse methodologies. At small scale, microscopy is often utilized but also a medical analysis technique such as magnetic resonance imaging (MRI) can be used to examine the accumulation of biomass and the biofilm

structure. MRI technique generates 3D images of the attached biofilm which, through further image processing, can be employed to obtain quantitative data such as the interfacial area and the volume. A similar approach was previously reported by Deshusses et al. (1998) who determined interfacial area and biofilm thickness in a BTF and a biofilter beds by Computerized Axial Tomography. The authors emphasized that the superficial area was higher than expected and it was related to biofilm roughness contribution and concluded that further analysis of other supports at different void fractions were needed.

At the reactor (macroscopic) dimension, pressure drop is usually evaluated as a response to biomass growth (or accumulated byproducts such as elemental sulfur, EPS, etc). Further assessment at this scale includes the evaluation of the residence time distribution technique (RTD), which has been used for characterizing the hydrodynamics in biotrickling filters (Iliuta et al. 2002; Trejo-Aguilar et al. 2005, Sharvelle et al. 2008a). It is often considered that the liquid movement through a porous bed occurs by an ideal plug flow pattern. Nonetheless some preferential channels or stagnant zones may arise as consequence of packing structure and heterogeneity of biofilm growth, thus giving place to axial dispersion. In this sense, RTD analysis provides a measure of liquid dispersion for circulating fluids in packed beds. Many models accounting for axial dispersion in trickle-bed reactors have been described (Shah 1979; Herskowitz & Smith 1983; Gianetto & Specchia 1992; Levenspiel 1998) being the piston dispersion model the simplest and the more easily used in design. Nevertheless the application of these expressions in modeling biotrickling filters is not common.

To date only few models include liquid dispersion to simulate gas treatment performance in biofilters and biotrickling filters (Zarook et al. 1998; Iliuta et al. 2002; Sharvelle et al. 2008b). Some other include interesting analyses through biomass growth functions to predict its influence on the biofiltration process (Alonso et al. 1996; Alonso et al. 1998; Iliuta et al. 2002). However these models were focused on packing particles with relatively simple geometries. Therefore further studies are needed to evaluate hydrodynamic features of recently used packings, such as open pore polyurethane foam (PUF), coupled with biofilm buildup to simulate their effects over the gas treatment in biotrickling filters.

The aim of the present work was to examine the biomass accumulation effects over a long-term operated BTF hydrodynamics and performance. This objective was attained by means of assessing the biological intrinsic kinetics of the biofilm, by evaluating the available space and interfacial area for gas treatment in the BTF bed packed with open polyurethane foam through advanced imaging techniques and by simulating biofiltration

performance using a mathematical model. Furthermore, a geometric model consisting in an orthogonal 3D mesh allowed representing the complex porous structure of polyurethane and predicting how the superficial area is affected as biomass increases and other hydrodynamic phenomena, such as reduced residence time or increased water hold up are altered.

Experimental

Biotrickling filter

A squared column (0.08 x 0.08 m) BTF with four separated modules (height = 0.12 m each) and five ports to sample gas or liquid (Fig. 1a) was used. It contained a total of 48 PUF cubes (0.04m x 0.04m x 0.04cm) as carrier material. Superficial area for this specific PUF is 480 m^2 m^{-3} according to manufacturer. The apparent density and porosity were determined in the laboratory and found to be 21 kg m^{-3} and 0.98 respectively. Colonized PUF cubes were extracted from a previous alkaline BTF that was operated for more than a year degrading efficiently DMDS concentrations below 140 ppmv with 40 s of empty bed gas residence time, where biofilm was well developed in all the support. Information about bacterial consortium, mineral medium and long term gas treatment performance can be found elsewhere (Arellano-García et al. 2012). The gas inlet and outlet were positioned in such a way that the BTF could operate either counter-current or in parallel flow mode. The BTF was provided with a spray nozzle that distributes the liquid uniformly over the transversal area. The liquid volume at BTF bottom (V_{LRES}) was 0.8 L. The gas and liquid flows (Q_G and Q_L) were set at 0.27 and 0.04 m^3 h^{-1} respectively to have a gas residence time of 40 s, and linear velocities of gas (u_G) and liquid (u_L) of 42.0 and 6.5 m h^{-1}. The pressure drop for the gas stream was measured with an U tube manometer filled with water.

(Here Fig. 1)

Intrinsic biological kinetics determination

Effective degradation rates without mass transfer effects were determined for biofilm in a liquid phase respirometer, which consisted of a jacketed 2.6 mL glass chamber equipped with magnetic agitation, temperature control at 30º C and a polarographic oxygen probe (YSI 5300A, USA). Biofilm samples were extracted from colonized PUF and milled in a glass pestle tissue grinder to eliminate macroscopic granules. The resultant slurry was washed twice with mineral medium to remove DMDS and then centrifuged to have a suspension which was used to evaluate biomass concentration. The respirometer was filled in batches with air

saturated mineral medium, a specific volume of biomass suspension and pulses of a concentrated DMDS aqueous solution. Specific oxygen consumption was registered as a function of DMDS and biomass protein concentration. The reaction rate of DMDS was evaluated based on biotic oxygen uptake rate and the oxidation stoichiometry reported by Smith & Kelly (1988) and shown in equation 1. Biological kinetics was estimated by minimizing the squared error between data from respirometry tests and the predictions of a Haldane type reaction model with inhibition by substrate.

$$CH_3\text{-}S\text{-}S\text{-}CH_3 + 6.5\ O_2 \rightarrow 2\ CO_2 + 2\ H_2SO_4 + H_2O \quad [1]$$

Trickling liquid flow pattern description

To characterize the liquid flow through the BTF, the liquid residence time distribution (RTD) technique was used. Dextran blue was utilized as tracer for the liquid stream as it is stable in time and pH. Its high molecular weight (20,000 g mol^{-1} approx.) hinders absorption in the biofilm and packing material. Tracer pulses volume was in all cases 4 mL with a concentration of 10 g L^{-1}. The pulses were injected into the liquid stream through a septum located upstream just before the spray nozzle. Liquid samples were collected at intervals between 4 and 10 seconds and their absorbance was measured within 1 h. The BTF dynamic liquid hold-up was obtained by measuring the liquid volume drained after 15 min of stopping gas and liquid flows.

The dispersed plug flow model equation for closed vessels (Eq. 2) was utilized to fit the experimental RTD curves and to determine dispersion coefficient values, as suggested by Levenspiel (1998) when the multiple samples method for collecting the tracer is used.

$$2\frac{D_{disp}}{u_L F} - 2\left(\frac{D_{disp}}{u_L F}\right)^2 \left(1 - e^{-uL/D_{disp}}\right) - \frac{\sigma^2}{\underline{t}^2} = 0 \quad [2]$$

Where σ (h) is the time distribution variance of data, $\underline{t}$ (h) flowing liquid average residence time, u_L (m h^{-1}) liquid superficial velocity, D_{disp} (m^2 h^{-1}) dispersion coefficient and F (m) the characteristic length (in this case the bed total height). Curves of tracer concentration in samples as function of time obtained as results from RTD experiments allowed the calculation of variance and average residence time. The Péclet number (Pe) for mass transfer was calculated as $(u_L \cdot F)/D_{disp}$. Total liquid hold-up, ϕ (m^3) was calculated by multiplying $\underline{t}$ by Q_L. Liquid film depth, L (m) was determined by dividing total liquid hold-up by the biofilm superficial area (a_b).

Biofilm physical features determination

The examination of the biofilm was performed between days 10 and 20 (see fig. 3). Biofilm volume in PUF was evaluated by extracting five packing pieces from the BTF. Afterwards the biomass from each piece was individually detached by successive washings and centrifuged to measure pellet volume. An average between all samples was calculated to have a representative value of biomass concentration throughout the BTF. Biofilm thickness (δ) was estimated by dividing the biomass volume by the clean packing superficial area (a_p).

Magnetic Resonance Imaging (MRI) analysis was applied to some of the colonized packing pieces. For this technique some carrier cubes were submerged in alkaline mineral medium mixed with gadolinium contrast agent (Gadovist, 1 mmol L^{-1}, Bayer, Mexico). Afterwards, the foam cubes were drained for 1 hour and then analyzed in a magnetic scanner (Varian, VNMR 7T, USA). Standard gradient-eco sequences (GEMS) were acquired in a 50 per 50 mm field with a 512x512 pixel matrix giving a resolution of 97.5 μm. Sequences of 80 images were acquired from each cube taking a slice image every 0.5 mm. Only the biofilm structure impregnated with the contrast medium was registered as the polyurethane matrix is invisible in this assay. Superficial area and volume of the biofilm were calculated from 3D reconstructions made with the OsiriX imaging software. Estimates of volume occupied either by total liquid hold-up and biofilm volume were deducted from packing material original void space to have an approximation of the actual bed porosity (ε).

Analytical methods

Biofilm protein content was measured by digestion in 0.2N NaOH and further analysis with a reagent kit assay (DC BioRad, USA). Gaseous DMDS concentration was analyzed using a gas chromatograph equipped with a FPD detector (HP 5890, USA) and a capillary column (Varian CP-PORABOND Q 25 m× 0.32 mm× 5 μm, USA). Sulfate was determined according to Standard Methods (1998). Dextran blue liquid concentration was evaluated by spectrophotometry at 290 nm (Jiménez et al. 1988). To evaluate gas treatment performance in the BTF, the elimination capacity, EC (g_{DMDS} $m^{-3}h^{-1}$), and removal efficiency RE (%), were calculated as

$$EC=\left[\left(C_{in}-C_{out}\right)/V_{bed}\right]\times Q_G \quad [3]$$

$$RE=\left[\left(C_{in}-C_{out}\right)/C_{in}\right]\times 100 \quad [4]$$

Where C_{in} and C_{out} (g_{DMDS} m^{-3}) are the inlet and outlet concentrations respectively, Q_G (m^3 h^{-1}) is the gas flow rate, and V_{bed} (m^3) is the packed bed volume.

Biofiltration model

The proposed model is based on the mathematical description of a BTF made previously by Kim and Deshusses (2003). The main assumptions are:

- The packing is completely covered by biofilm, which is in turn entirely coated by a liquid film.
- Gas flow is considered to be plug flow while the axial dispersion model describes the liquid flow.
- Gas-liquid and liquid-biofilm interphases are in equilibrium, according to Henry law constants.
- The biodegradation reaction occurs only in the biofilm and it was not limited by oxygen.

The following partial differential equations describe the dynamic mass balances expressed in concentration (C). Mass balances for oxygen and DMDS (both gaseous and dissolved) and sulfate (dissolved) were calculated in gas, liquid and biofilm phases considered for BTF modeling. Mass balances for DMDS are depicted in equations 5 to 9. The subscripts G, L, B and REC denote gas, liquid, biofilm and recirculation, while iG and iB indicate the gas-liquid and liquid-biofilm interfaces respectively.

Gas phase

$$\frac{\partial C_G}{\partial t} = u_G \frac{\partial C_G}{\partial z} - \frac{k_L a_b}{\varepsilon}\left[\left(C_G/H\right) - C_L\right] \qquad [5]$$

Where u_G is the gas superficial velocity in the BTF and H is the dimensionless Henry law constant. Initial condition at t=0, $C_G=0$. Boundary condition at discretization i=1, $C_G=C_{in}$, either for counter current or parallel flow mode, (see fig. 1b).

Liquid phase

$$\frac{\partial C_L}{\partial t} = -D_{disp}\frac{\partial^2 C_L}{\partial z^2} + u_L \frac{\partial C_L}{\partial z} + \frac{k_L a_b}{\phi}\left[\left(C_G/H\right) - C_L\right] - \frac{a_b D_{eff}}{L}\left[C_{L(iG)} - C_{L(iB)}\right] \qquad [6]$$

Where u_L is the superficial liquid velocity inside the BTF. Initial condition at t=0, $C_L=0$. Boundary conditions: for counter current flow $C_L=C_{LREC}$ at i=10. For parallel flow $C_L=C_{LREC}$ at i=1. In any case for i=1 to 10, $C_L=C_G/H$.

Biofilm

$$\frac{\partial C_B}{\partial t} = \frac{D_{eff}}{\delta^2}\frac{\partial^2 C_B}{\partial x^2} - R_B \qquad [7]$$

Where Deff is the diffusion coefficient for DMDS. Initial condition at t=0, C_B=0. Boundary condition at biofilm-liquid interface j=1, C_B=C_L; while at biofilm-support interface $\partial C_B / \partial x = 0$.

Biological reaction kinetics

$$R_B = R_{max} \frac{C_B}{C_B + K_S + C_B^2 / K_i} \quad [8]$$

Balance for the recirculating liquid at BTF bottom

$$\frac{\partial C_{LREC}}{\partial t} = \frac{Q_L}{V_{LREC}} \left(C_L - C_{LREC} \right) \quad [9]$$

Initial condition at t=0, C_{LREC}=0.

Either ideal or dispersed plug flow for liquid was considered in the model to solve the mass balances in the liquid phase. The difference between these two flow patterns is based on the supposition that the velocity profile for the liquid through the BTF porous bed is plug flow or a certain degree of retro mixing is present in the plug front (dispersed) inducing irregularities in the velocity profile without leading to stagnant zones or channeling. In the latter case the dispersion term in eq. 6 is added to the liquid phase mass balance. Model equations were solved with the Matlab® software using the finite differences method. For this procedure, both BTF packed height and biofilm thickness were discretized in ten sections each for simulation (see Fig. 1b). Increasing the discretization number did not change significantly the model estimations.

Polyurethane foam model

The complex internal structure of the polyurethane foam was simplified according to figure 2 in order to examine the effect of biofilm growth on superficial area and void space.

(Here Fig. 2)

The foam, figure 2a, was approximated by a tridimensional orthogonal mesh formed by cylindrical PUF filaments as in figure 2b. The number and diameter of the filaments in the mesh were adjusted by fitting to the experimentally obtained values of the apparent density (21±0.5 kg m^{-3}) and the filament diameter (0.3±0.1 mm) of the foam used in our assays. The intersections of the filaments (figure 3c) implied superficial area and volume losses due to superposition of plastic segments and biofilm. These reductions were accounted in the

model considering each node to have the shape of the well-known Steinmetz solid, which is formed by the orthogonal intersection of three cylinders. The area and volume of the Steinmetz solid were calculated as:

$$A_{st} = 3/4\,(16-8\sqrt{2})D^2 \quad [10]$$

$$V_{st} = (2-\sqrt{2})D^3 \quad [11]$$

Where D corresponds to the diameter of a single filament; the matrix superficial area and volume of a $1m^3$ basis were then calculated as:

$$a_{sp} = \left(NF \cdot \pi \cdot D \cdot \lambda\right) - \left(3 \cdot NI \cdot A_{st}\right) \quad [12]$$

$$V_{sp} = \left(NF \cdot \pi \cdot 1/4\,D^2 \cdot \lambda\right) - \left(2 \cdot NI \cdot V_{st}\right) \quad [13]$$

Where NF is the number of filaments, NI is the number of intersections and λ represents the longitude of filaments, in this case equivalent to 1m. The effect of biofilm development over the superficial area and biomass volume was evaluated by supposing a uniform biofilm growth on the filaments and thus the diameter in equations 10-13 and figure 2c. Biofilm volume estimates were corrected by subtracting the volume of the biofilm-free filament considering the diameter in Table 1.

Results

Gas treatment performance in the biotrickling filter

During the period of the experiments reported here, the BTF maximum elimination capacity (EC) was 20 $g_{DMDS}\ m^{-3}\ h^{-1}$, with removal efficiency (RE) of around 86% as it is shown in figure 3. Concentration of sulfate as the end product of degradation was kept below 10 g L^{-1} to avoid the inhibition on performance previously observed (Arellano-García et al., 2012). The pressure drops were 1.9 and 4.0 $cm_{H2O}\ m_{column}^{-1}$ (0.2 and 0.4 kPa m_{column}^{-1}) for parallel and countercurrent mode respectively.

(Here Fig. 3)

Polyurethane foam model

Mathematical optimization of the number of filaments in the matrix fitting the experimentally measured packing apparent density of 21 kg m^{-3} lead to the results presented in table 1.

(Here Table 1)

With data in table 1 as the starting point, the superficial area and the volume occupied by the biofilm were estimated using equations 10-13 and varying D which is related to the biofilm depth and the results are depicted in figure 4. The irregular bell shape curve predicts initially an increase in the specific area as the biofilm is formed on the filaments by the effect of increased diameter. As the diameter increases, in this case beyond a biofilm depth of around 0.7 mm, the superficial area diminishes due to the increase of the node size (Fig. 2c and eq. 12).

(Here Fig. 4)

Biofilm physical features

Five PUF colonized cubes were sampled between day 10 and 20 (see fig. 3) and by detaching the biofilm it was found that 30±2% of the packed bed volume (0.9 L) was occupied by biomass. After dividing this volume by the superficial area of the clean PUF an average biofilm thickness of 0.6±0.1 mm was calculated. Further analyses of packing cubes but now with MRI showed a coarse biofilm surface (see Fig. 5) and further image analysis suggested that the biomass occupied approximately 35% of bed volume while its superficial area was around 650 m^2 m^{-3}. An animation of the reconstructed images This was similar to the sum of volume percentage calculated by detaching the biomass plus the 2.0% of the PUF packing volume occupied by polyurethane itself.

(Here Fig. 5)

Intrinsic biological kinetics

Figure 6 shows the results of the intrinsic oxygen uptake rates from respirometry experiments. The DMDS consumption was correlated by means of equation 1 and served to fit the reaction model (eq. 5) which is represented in figure 6. Considering a protein to biomass ratio of 0.3 w/w (González-Sánchez et al. 2008), values of 3571.6 g_{DMDS} $m^{-3}_{biofilm}$ h^{-1}, 2.7 g_{DMDS} m^{-3} and 8.2 g_{DMDS} m^{-3} were determined for R_{max}, K_s and K_i respectively.

(Here Fig. 6)

Trickling liquid flow description

Figure 7 shows the RTD profiles obtained for the liquid flow through the BTF packed bed. It is observed that tracer elution through clean PUF is faster than through colonized PUF as a result of higher liquid hold up and the tortuosity promoted by biofilm growth. Therefore average liquid residence times through clean and colonized PUF were 10 and 60 s respectively. In both cases complete recovery of tracer was verified by mass balances in liquid flow, thus discarding tracer absorption in either biofilm or PUF. By observing the trickling liquid at the bottom of the modules, it was found that biomass growth favors the redistribution of the liquid through the packing.

(Here Fig. 7)

Main results from RTD experiments for flow through clean and colonized PUF are shown in table 2. The Péclet number was determined after adjusting the distribution time data to the closed vessel model (eq. 2).

(Here Table 2)

Biotrickling filter model

Table 3 shows a summary of the parameters introduced in the BTF model for simulate gas treatment. With these parameters, model predictions of concentration profiles with both variations (ideal and disperse plug flow), either in counter current or parallel flow operation, were compared with experimental data and the results are depicted in figure 8. Similar comparison was made with an independent experiment but with an initial concentration of 0.25 g m^{-3} (not shown) with trends similar to those found in Fig. 8.

(Here Table 3)

(Here Fig. 8)

Discussion

As it is observed in figure 6, results from respirometry fit well a Haldane reaction model with inhibition by substrate. Nonetheless it is possible to consider that no inhibitory effect of DMDS would be present at the BTF operation conditions reported here where initial gaseous concentrations never exceeded 140 ppmv (0.54 g m^{-3}). On the contrary, the amount of gaseous DMDS employed in this study promoted liquid concentrations where maximum reaction rate would be located. Compared to kinetics previously reported for DMDS oxidizing bacteria in neutral cultures (Smith & Kelly, 1988), the alkaliphilic biofilm in this study showed smaller DMDS affinity and degrading activity of one and two orders of magnitude respectively. Far from

being considered as a drawback, this may imply an advantage for the alkaliphilic biomass in biofiltration applications where, considering that growing is directly related to microbial activity, a slow colonization of packing material would lengthen the time before bed channeling or plugging to be present, while microbial activity is enough to carry out low DMDS concentrations removal satisfactorily. In this sense the observed DMDS elimination capacities during the experiments reported here (fig. 3), are comparable with previous reports of DMDS treatment in BTF at neutral pH (Ramirez et al. 2011, Wan et al. 2011). However it is important to consider that in our case the effective gas residence time was reduced approximately to half of that initially calculated (40 s), due to biomass accumulation and liquid hold-up presence.

In a previous experiment (data not shown), detaching approximately 0.3 L of biomass from the packing lead to an EC increase of nearly 50%. Nonetheless, it was observed a liquid hold-up increase from 20 to 30%. The increased elimination capacity obtained in the BTF operation after detaching part of the immobilized biomass may be a consequence of a higher superficial area available for DMDS absorption, nonetheless this extra area would be equally covered with a trickling liquid film as indicated previously (Picioreanu et al. 2000) explaining the liquid hold-up increase observed after detaching part of the biofilm.

From RTD experiments (fig. 7), it is seen that biomass accumulation in PUF support leads to an increment of liquid retention time in accordance to results previously reported by other authors (Trejo-Aguilar et al. 2005; Sharvelle et al. 2008a) where the presence of stagnant zones was emphasized. In our case the intricate porous structure of PUF may influence the liquid flow pattern even when biomass was absent, obtaining Péclet values of 10.3 and 4.3 for liquid flow through clean and colonized PUF respectively. Having in mind that ideal plug flow is characterized by Pe magnitudes higher than 100 (Levenspiel 1998), it is clear that the dispersion degree is substantial for the liquid flow through PUF at any colonization stage.

As it is portrayed in figure 8 the dispersed plug flow model (DPFM) fits better the experimental data than the ideal plug flow model (IPFM), especially when predicting the performance in parallel flow mode. The contrast between DPFM and IPFM shows that dispersion for liquid streams should be considered when modeling BTFs operation, at least when materials similar to open polyurethane foam are used. With respect to the flow mode operation, it was observed experimentally that when BTF was operated in parallel flow mode both smaller liquid hold-up (see table 2) and pressure drop were obtained as compared to counter current flow. This result evidences the interaction between gas and liquid flow direction and suggests that parallel

operation may be a better choice at least from the energy consumption point of view. In any case the biofiltration model showed that no limitation by oxygen occurred within the biofilm, although it may not be discarded that actual liquid O_2 concentrations are lower than calculated due to endogenous respiration.

In relation to the real PUF comparison to the mesh model proposed in this study, the main differences arise from the complexity and randomness of real packing, which could promote biomass growth similar to that observed on the MRI images (fig. 5a and b and video). Some PUF estimated properties as average pore size and porosity were in well agreement with measured values. Others, such as the predicted superficial area, was about half of what was reported by manufacturer. This difference may be attributable to the limitations in the definition and implementation of the relatively simple model and real structure of PUF, in this sense heterogeneity of filaments width and tortuosity may provide important amounts of superficial area.

Regarding to estimated properties from mesh model, the predicted superficial area for clean PUF was close to 220 m^2 m^{-3} and would rise as a function of biofilm growth until attaining a maximum near 620 m^2 m^{-3}, where close to 30% of packing would be occupied by biomass (fig. 4). From this point on specific area diminishes as consequence of further biofilm accumulation. In this respect, a mathematical representation of a biofilter with specific area dependence on biofilm growth was previously reported (Alonso et al. 1998). These authors considered spherical geometry for packing particles and model predictions respecting pollutant removal were in well agreement with experimental data, however the estimated specific area was invariably decreasing since theoretical biofilm development began. In contrast the physical model for superficial area utilized in this study led to a bell curve type function (fig. 4), which fits to scatter data either from foam manufacturer and MRI determination and may serve as evidence of this area tendency actually being happening when PUF is colonized in a biotrickling filter.

Furthermore when estimated values of superficial area depicted in figure 4 were introduced into the biotrickling filter model the influence of biomass accumulation over gas residence time and treatment efficiency of the alkaline BTF treating DMDS vapors was estimated and the results are illustrated in figure 9.

(Here Fig. 9)

As shown in figure 9, when volume occupied by biomass increased from 0 to 20%, the specific area also augments from 220 to 570 m^2 m^{-3}; nevertheless RE shows an increment of barely 15%. This predicted low response in RE when superficial area increases more than 150%, may be a consequence of a process

limitation by reaction in biofilm. In this regard it would be expected that further biomass accumulation lead to higher RE values. Nonetheless, model shows the opposed with an ER drop when biomass occupied 32% of bed volume in spite of area reaching 615 m^2 m^{-3}. This could be attributable to the gas residence time reduction, which at this point would be 60% of its initial value. Thereafter the RE diminishing tendency remains as it is driven by reductions in gas residence time and superficial area.

Images obtained from the MRI analysis showed a biomass structure that agreed with previous reports (De Beer et al. 1993; Lewandowski et al. 1995) where the biofilm roughness was described. This could lead to superficial area increments and hydrodynamic changes influencing the gas treatment performance in practical applications. In this sense the biofilm structure effect on mass transport was theoretically addressed by Picioreanu et al. (2000) emphasizing that even when coarseness could lead to a biofilm area rise, effective mass transfer may decrease as only biofilm peaks receive substrate while valleys remain filled with stagnant liquid that hinders substrate diffusion. Therefore the liquid velocity through biomass irregularities is highlighted as a determining factor for mass transport through a gas liquid interface. This reasoning could be directly related with experimental evidence in biofiltration applications where liquid flow rate has a greater impact over performance compared to gas speed changes (Diks & Ottengraf 1991a, b).

The agreement between the BTF bed volume occupied by biofilm either evaluated by manually detaching the biofilm and by MRI analysis indicates the possibility of determining some specific parameters with relatively simple procedures. However, further comparisons at different colonized volume fractions and packing materials are required to confirm this evidence.

The theoretical analysis for BTF performance carried out in this study locates the optimum biomass concentration near 20% of bed volume, which would correspond to a biofilm depth of 0.4 mm immobilized on PUF surface. At this condition RE close to 90% would be expected with gas residence time reductions no higher than 30% while pressure drop would be close to 0.5 cm H_2O m_{column}^{-1} as it was calculated from the Darcy law equation; this would imply low energy requirements for compressing the gas stream for feeding a biotrickling filter.

In conclusion, the experimental procedures presented in this study were utilized to evaluate parameters which are rarely assessed when colonized supports in a biotrickling filter show extensive microbial growth. These

features included gas residence time, superficial area and dispersion degree in the liquid stream which proved to be closely influenced by biomass accumulation.

With the aid of experimentally determined parameters, the effect of biomass growth on performance of a biotrickling filter was obtained by coupling a simple, yet powerful, representation of the complex PUF topology using an orthogonal mesh to the usual mass balance equations. Model predictions emphasized the relative importance of biotic (such as biomass content and degradative activity) and abiotic (superficial surface, effective residence time, etc) parameters on performance. Thus at first stages after startup, modeling predicts biomass concentration to be the biofiltration limiting factor, while at high biomass accumulations, typical of a long term operation, reduced residence time could determinate the gas treatment efficiency. Furthermore, this theoretical analysis permitted to establish an optimum biomass concentration which could be maintained more easily with a slow growing microbial consortium as alkaliphilic bacteria, while acceptably removal rates of gaseous pollutant would be obtained. It can be predicted that other systems may require less biomass if the specific activity is higher than the consortium used here. Characterization of the biofilm may be performed repeatedly throughout BTF operation to obtain valuable information about the relationship between biofilm growth and gas treatment performance.

Acknowledgements

To Conacyt for financing this project (I0017-166451) and the scholarship of LAG. And also to AECID for granting the funds for LAG internship in the UPC-Barcelona. To the CI3M center of UAM-Iztapalapa for images.

References

Alonso C, Suidan MT, Sorial GA, Smith FL (1996) Gas Treatment in trickle-bed biofilters: biomass, how much is enough? Biotechnol Bioeng 54(6):583-594.

Alonso C, Suidan MT, Kim BR, Kim BJ (1998) Dynamic mathematical model for the biodegradation of VOCs in a biofilter: biomass accumulation study. Environ Sci Technol 32:3118-3123.

Arellano-García L, González-Sánchez A, Van Langenhove H, Kumar A, Revah S (2012) Removal of odorant dimethyl disulfide under alkaline and neutral conditions in biotrickling filters. Water Sci and Technol 66(8):1641-1646.

Bonilla WC, (2013) Uso de respirometrías heterogéneas para estimar coeficientes de transferencia de masa interfaciales y parámetros biocinéticos en biofiltros de lecho escurrido. Dissertation, UAM Iztapalapa, México.

De Beer D, Stoodley P, Roe F, Lewandowski Z (1993) Effects of biofilm structures on oxygen distribution and mass transport. Biotechnol Bioeng 43(11):1131-1138.

Deshusses MA, Cox HHJ, Miller DW (1998) The use of CAT scanning to characterize bioreactors for waste air treatment. Paper 98-TA20B.04. In: Proceedings Annual Meeting and Exhibition of the Air and Waste Management Association, San Diego, CA, USA.

Diks RMM, Ottengraf, SPP (1991a) Verification studies of a simplified model for the removal of dichloromethane from waste gases using a biological trickling filter (Part I). Bioprocess Eng 6:93-99.

Diks RMM, Ottengraf, SPP (1991b) Verification studies of a simplified model for the removal of dichloromethane from waste gases using a biological trickling filter (Part II). Bioprocess Eng 6:131-134.

Dorado AD, Lafuente J, Gabriel D, Gamisans X (2012) Biomass accumulation in a biofilter treating toluene at high loads. Part 2: Model development, calibration and validation Chem Eng J 209: 670-676.

Estrada JM, Kraakman NJR, Lebrero R, Munoz R (2012) A sensitivity analysis of process design parameters, commodity prices and robustness on the economics of odour abatement technologies. Biotechnol Adv 30:1354-1363.

Gianetto A, Specchia V (1992) Trickle-bed reactors: state of art and perspectives. Chem Eng Sci 47(13): 3197-3213.

González-Sánchez A, Revah S, Deshusses MA (2008) Alkaline biofiltration of H_2S odors. Environ Sci Technol 42:7398-7404.

Herskowitz M, Smith JM (1983). Trickle bed reactors: A review. AIChE J 29(1): 1-18.

Iliuta I, Bildea SC, Iliuta MC, Larachi F (2002) Analysis of trickle bed and packed bubble column bioreactors for combined carbon oxidation and nitrification. Braz J Chem Eng 19(1):69-88.

Integrated Computer Aided System (ICAS), Educational Version. Computer Aided Process Engineering Center. Technical University of Denmark.

Jiménez B, Noyola A, Capdeville B (1988) Selected dyes for residence time distribution evaluation in bioreactors. Biotechnol Tech 2(2):77-82.

Kim S, Deshusses MA (2003) Development and experimental validation of a conceptual model for biotrickling filtration of H_2S. Environ Prog 22(2):119-128.

Levenspiel, O (1998) Chemical reaction engineering. John Wiley & Sons, New York.

Lewandowski Z, Stoodley P, Altobelli S (1995) Experimental and conceptual studies on mass transport in biofilms. Wat Sci Tech 31(1):153-162

Picioreanu C, van Loosdrecht MCM, Heijnen JJ (2000) A theoretical study on the effect of surface roughness on mass transport and transformation in biofilms. Biotechnol Bioeng 68(4):355-369.

Ramírez M, Fernández M, Granada C, Le Borgne S, Gómez JM, Cantero D (2011) Biofiltration of reduced sulphur compounds and community analysis of sulphur-oxidizing bacteria. Bioresource Technol 102:4047-4053.

Shah YT (1979) Gas-fluid-solid reactor design. McGraw-Hill International Book Co.

Sharvelle S, McLamore E, Banks MK (2008a) Hydrodynamic characteristics in biotrickling filters as affected by packing material and hydraulic loading rate. J Environ Eng-ASCE 134:346-352.

Sharvelle S, Arabi M, McLamore E, Banks MK (2008b) Model development for biotrickling filter treatment of graywater simulant and waste gas. I. J Environ Eng-ASCE 134:813-825.

Silva J, Morales M, Cáceres M, Morales P, Aroca G (2012) Modelling of the biofiltration of reduced sulphur compounds through biotrickling filters connected in series: effect of H_2S. Electron J Biotechn 15(3):1-15.

Smet E, Van Langenhove H (1998) Abatement of volatile organic sulfur compounds in odorous emissions from the bio-industry. Biodegradation 9:273-284.

Smith N, Kelly DP (1988) Isolation and physiological characterization of autotrophic sulphur bacteria oxidizing dimethyl disulphide as sole source of energy. J Gen Microbiol 134:1407-1417.

Standard Methods for the Examination of Water and Wastewater, 1998. 20th edn, American Public Health Association/American Water Works Association/Water Environment Federation, Washington, DC, USA.

Trejo-Aguilar G, Revah S, Lobo R (2005) Hydrodynamic characterization of a trickle bed air biofilter. Chem Eng J 113:145-152.

Wan, S, Li, G, An, T, Guo, B (2011) Co-treatment of single, binary and ternary mixture gas of ethanethiol, dimethyl disulfide and thioanisole in a biotrickling filter seeded with *Lysinibacillus sphaericus* RG-1. J Hazard Mater 186, 1050–1057.

Zarook SM, Shaikh AA, Azam SM (1998) Axial dispersion in biofilters. Biochem Eng J 1(1):77-84.

Figure captions

Fig. 1 a) Diagram of the biotrickling filter for DMDS treatment. 1 Needle valve. 2 Rotameter. 3 Peristaltic pump. 4 DMDS bubbling vessel. 5 Mixing vessel. 6 Packed bed. 7 Sodium hydroxide 1N solution. 8 pH control. 9 Exhaust gas extractor. b) Reactor bed discretization used for modeling

Fig. 2 Photography of the polyurethane foam used in this study, scale below is in centimeters (a), basic structure proposed for PUF physical model (b) and close up of a three filament intersection covered with biofilm (c)

Fig. 3 Biotrickling filter performance evolution during the experimental period. The reactor had been previously operated for over a year

Fig. 4 Specific area volume as functions of biofilm depth, on the model support depicted in figs. 2b and 2c

Fig. 5 a) Original MRI biofilm image in one 4cm-sided packing cube, b) 3D reconstruction of biofilm in a packing cube, c) close up of a biofilm portion and surface meshing for calculating interfacial area

Fig. 6 Alkaline biomass oxygen consumption rates as function of DMDS liquid concentration and fitting to the proposed reaction model (equation 8)

Fig 7 Tracer concentration profiles acquired during DTR experiments. Vertical arrows indicate mean residence time

Fig. 8 Experimental and simulated concentration profiles of DMDS along BTF height, for counter current operation (a) and co-current operation (b) for an initial gaseous DMDS concentration close to 0.30 g_{DMDS} m^{-3}

Fig. 9 Theoretical evaluation of biomass accumulation effect over superficial area, removal efficiency (RE) and gas residence time reduction in a BTF treating 27 g_{DMDS} m^{-3} h^{-1}, compared to experimental RE data (Δ) at same inlet load

Figure captions

Fig. 1 a) Diagram of the biotrickling filter for DMDS treatment. 1 Needle valve. 2 Rotameter. 3 Peristaltic pump. 4 DMDS bubbling vessel. 5 Mixing vessel. 6 Packed bed. 7 Sodium hydroxide 1N solution. 8 pH control. 9 Exhaust gas extractor. b) Reactor bed discretization used for modeling

Fig. 2 Photography of the polyurethane foam used in this study, scale below is in centimeters (a), basic structure proposed for PUF physical model (b) and close up of a three filament intersection covered with biofilm (c)

Fig. 3 Biotrickling filter performance evolution during the experimental period. The reactor had been previously operated for over a year

Fig. 4 Specific area volume as functions of biofilm depth, on the model support depicted in figs. 2b and 2c

Fig. 5 a) Original MRI biofilm image in one 4cm-sided packing cube, b) 3D reconstruction of biofilm in a packing cube, c) close up of a biofilm portion and surface meshing for calculating interfacial area

Fig. 6 Alkaline biomass oxygen consumption rates as function of DMDS liquid concentration and fitting to the proposed reaction model (equation 8)

Fig 7 Tracer concentration profiles acquired during DTR experiments. Vertical arrows indicate mean residence time

Fig. 8 Experimental and simulated concentration profiles of DMDS along BTF height, for counter current operation (a) and co-current operation (b) for an initial gaseous DMDS concentration close to 0.30 $g_{DMDS}\ m^{-3}$

Fig. 9 Theoretical evaluation of biomass accumulation effect over superficial area, removal efficiency (RE) and gas residence time reduction in a BTF treating 27 $g_{DMDS}\ m^{-3}\ h^{-1}$, compared to experimental RE data (Δ) at same inlet load

Table 1

Table 1. Estimated properties for the clean polyurethane foam.

Parameter	Estimated magnitude
Apparent density of matrix	21 kg m^{-3}
Filament diameter (D)	0.30 mm
Total filaments per m^{-3} (NF)	$2.55x10^{5}$
Total intersections per m^{-3} (NI)	$2.49x10^{7}$
Total filaments per linear meter	292
Pores per linear meter	291
Pore size	3.1 mm
Porosity	98 %
Superficial specific area	225 m^{2} m^{-3}

Table 2. Characteristic parameters for liquid flow through packed beds, obtained from RTD experiments.

Parameter (units)	Clean PUF	Colonized PUF
Liquid hold up, total (L)	0.1	0.6
Liquid hold up to bed ratio, v/v (%)	4	20
Dynamic hold up (L)	0.1	0.3
Liquid film depth (μm)	50	300
Dispersion coefficient (m^2 h^{-1})	0.30	0.72
Péclet number (dimensionless)	10.3	4.3

Table 3. Main parameters used in the biofiltration model.

Parameter	Value	Reference
DMDS Henry's law dimensionless constant (H)	0.061	Arellano et al., 2012
Biofilm thickness (δ)	0.6 mm	This study
Liquid film thickness (L)	0.2 mm	This study
Bed porosity during BTF operation (ε)	0.47	This study
Dispersion coefficient (D_{disp})	0.72 $m^2\ h^{-1}$	This study
DMDS diffusion coefficient (D_{eff})	$3.7x10^{-6}$ $m^2\ h^{-1}$	ICAS
Gas to liquid mass transfer coefficient, liquid side ($k_L a_b$)	26.4 h^{-1}	Bonilla, 2013
Biofilm superficial area (a_b)	650 $m^2\ m^{-3}$	This study
Specific max. DMDS uptake rate (R_{max})	3571.6 g $m^{-3}_{biofilm}\ h^{-1}$	This study
Saturation constant (K_s)	2.7 g m^{-3}	This study
Inhibition constant (K_i)	8.2 g m^{-3}	This study

Figure 1
Click here to download high resolution image

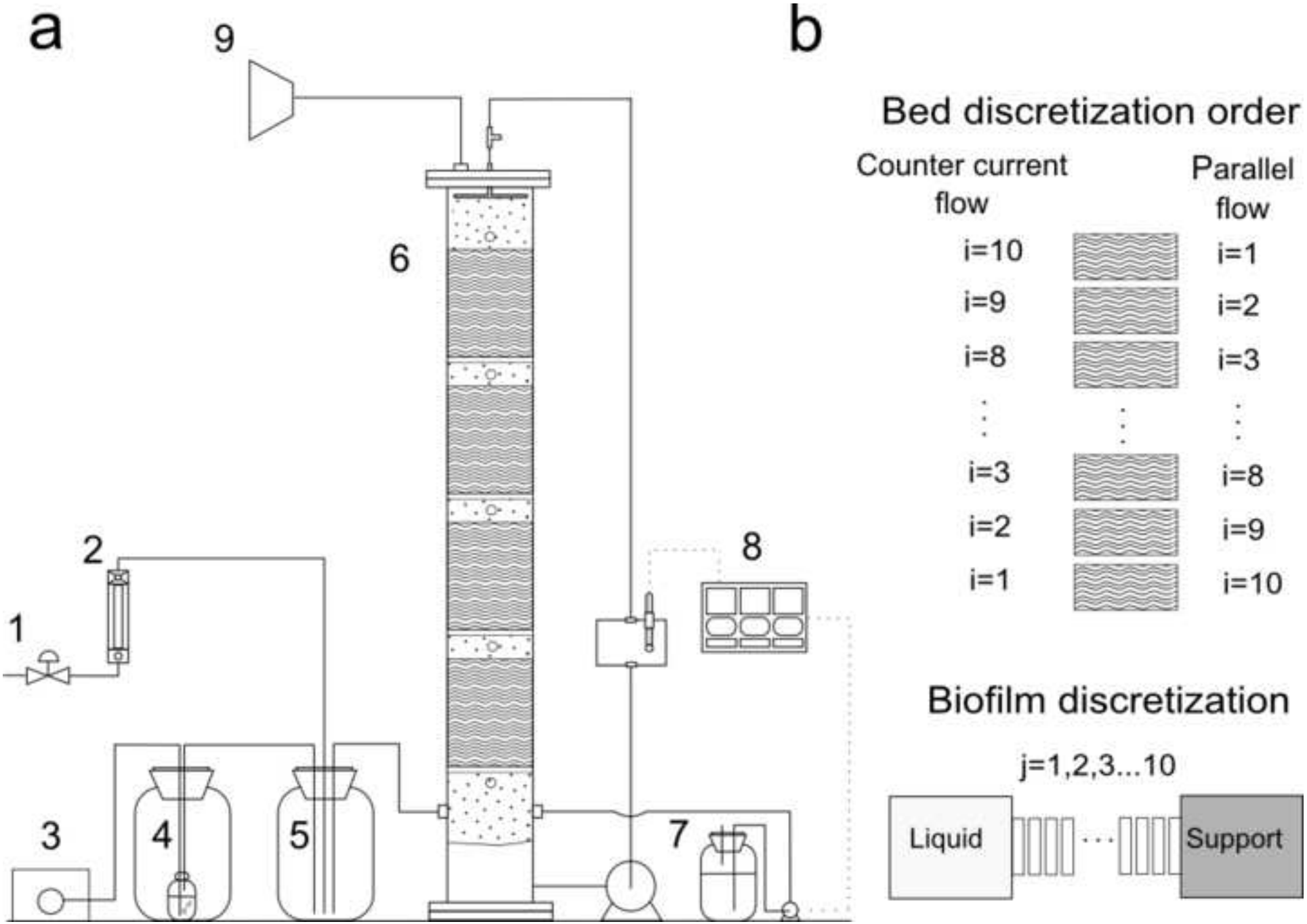

Figure 2
Click here to download high resolution image

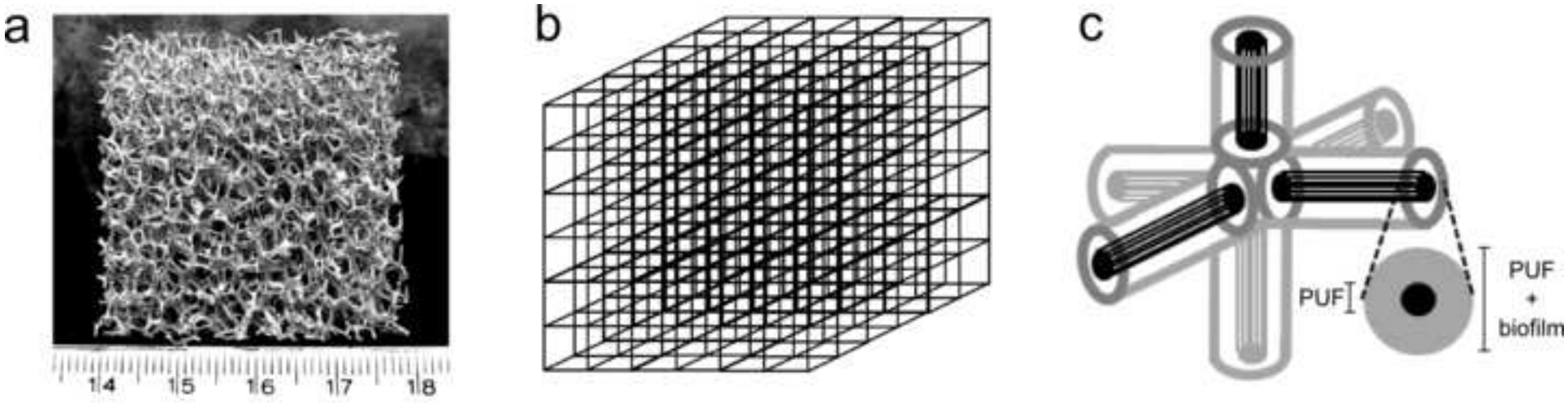

Figure 3
Click here to download high resolution image

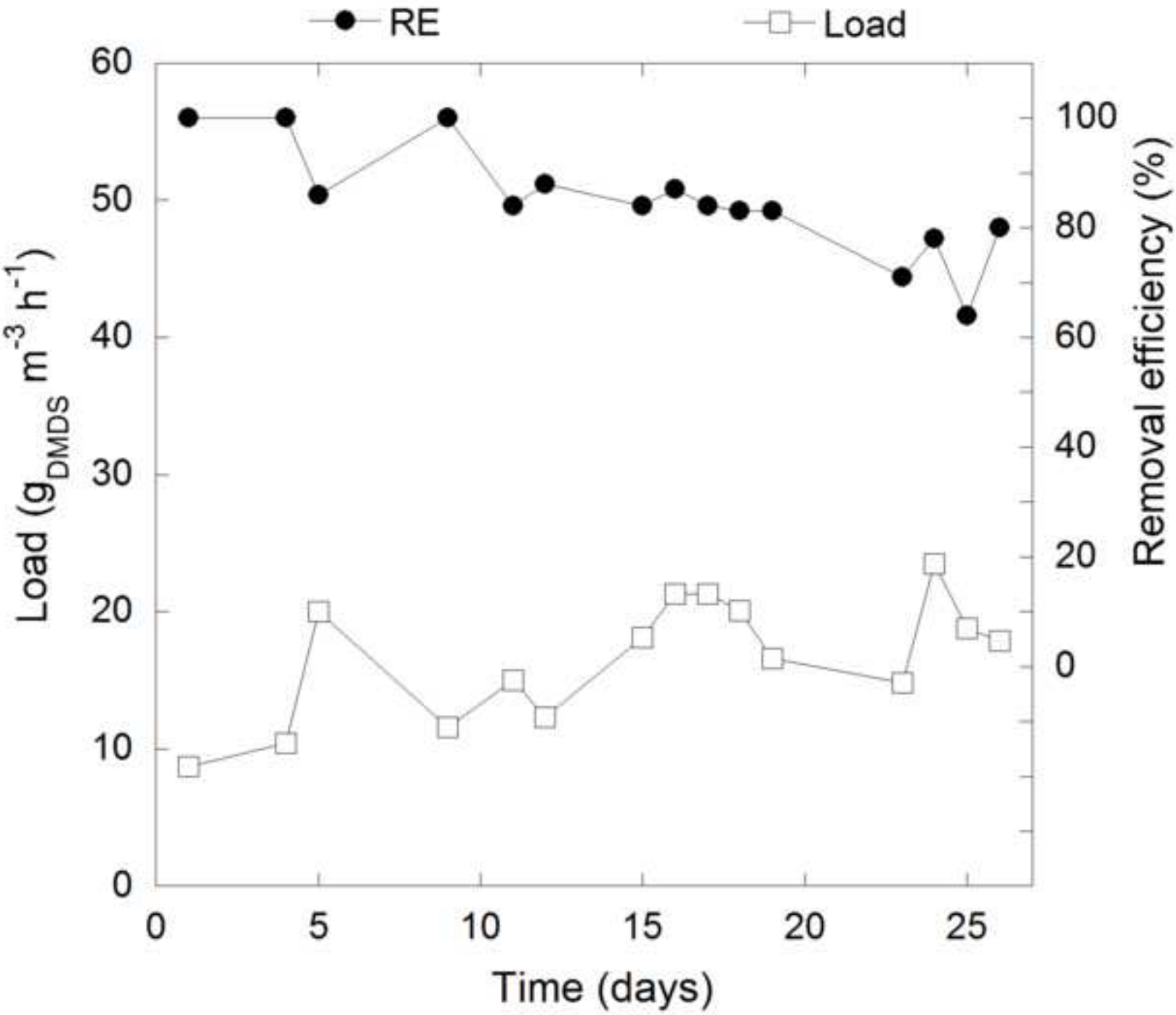

Figure 4
Click here to download high resolution image

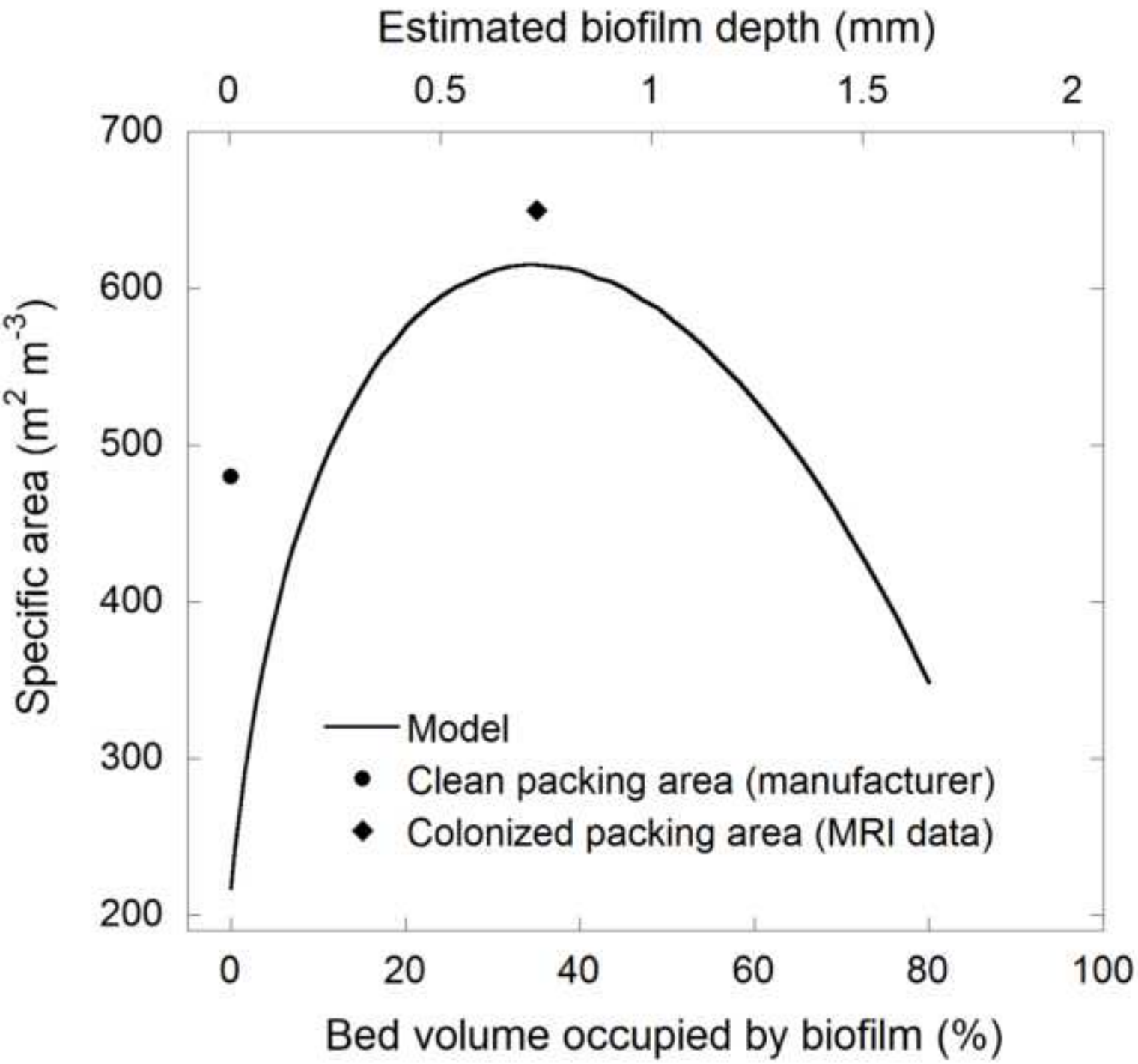

Figure 5
Click here to download high resolution image

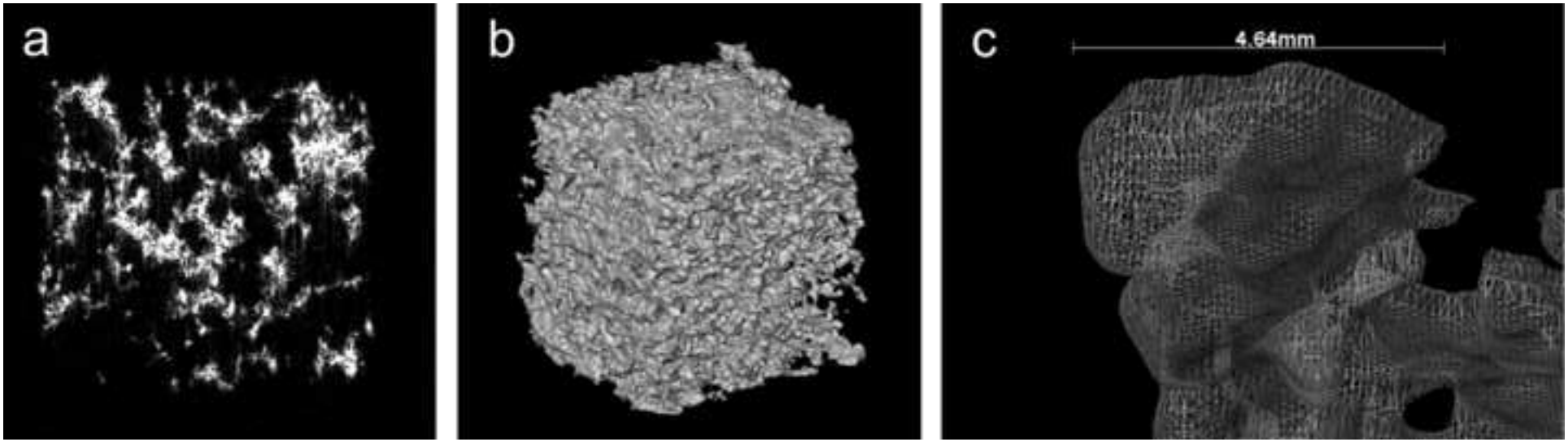

Figure 6
Click here to download high resolution image

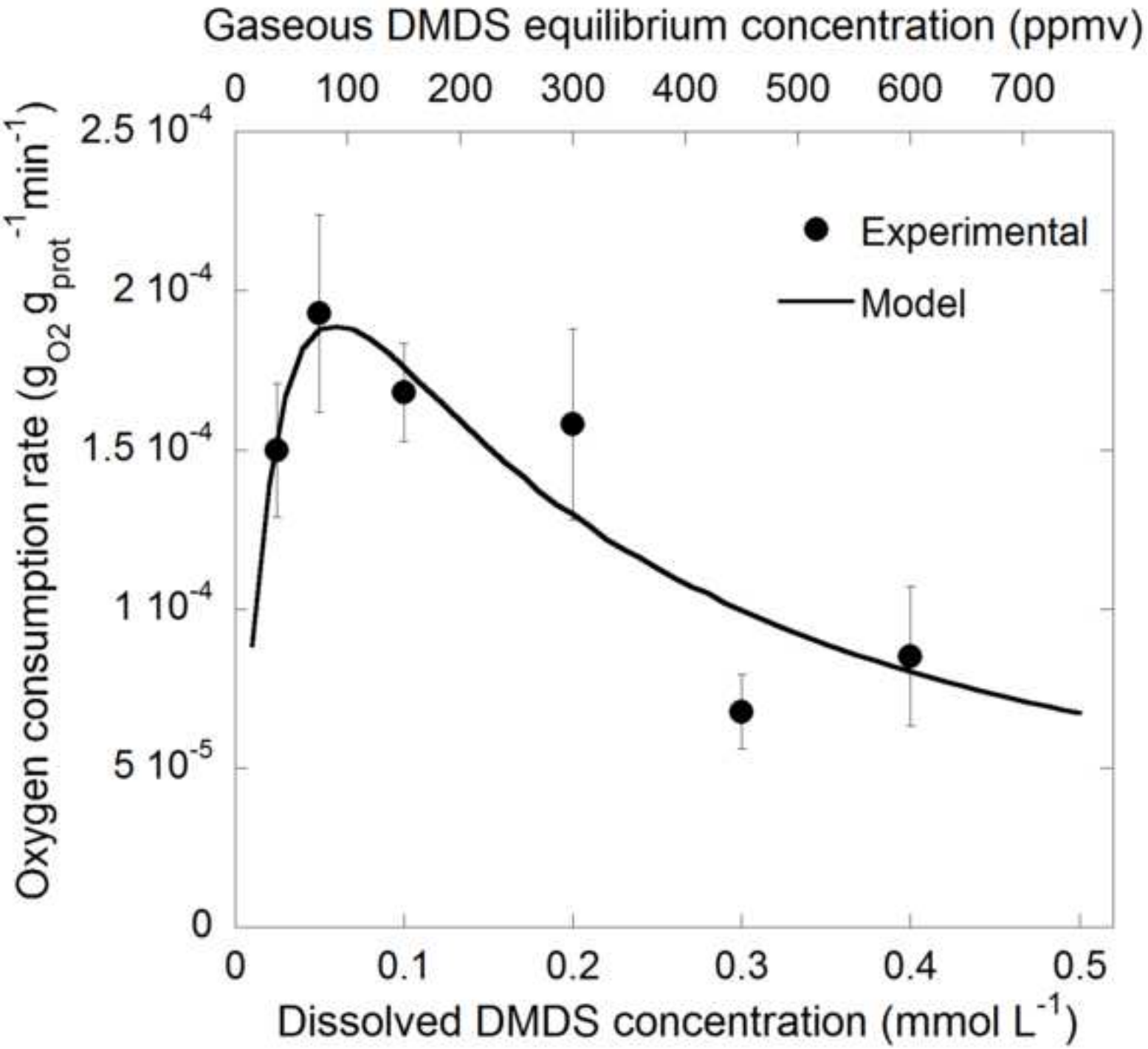

Figure 7
Click here to download high resolution image

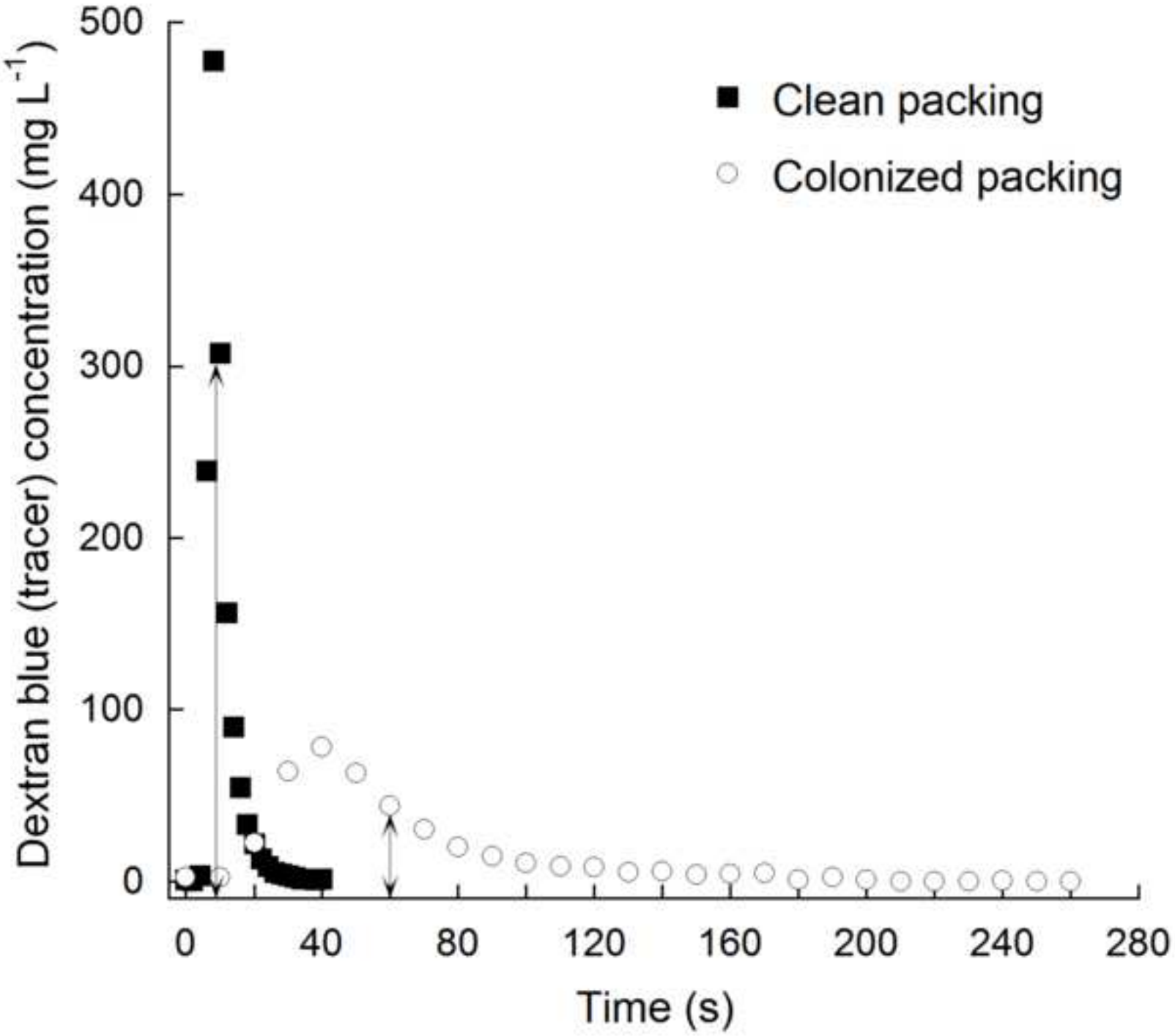

Figure 8
Click here to download high resolution image

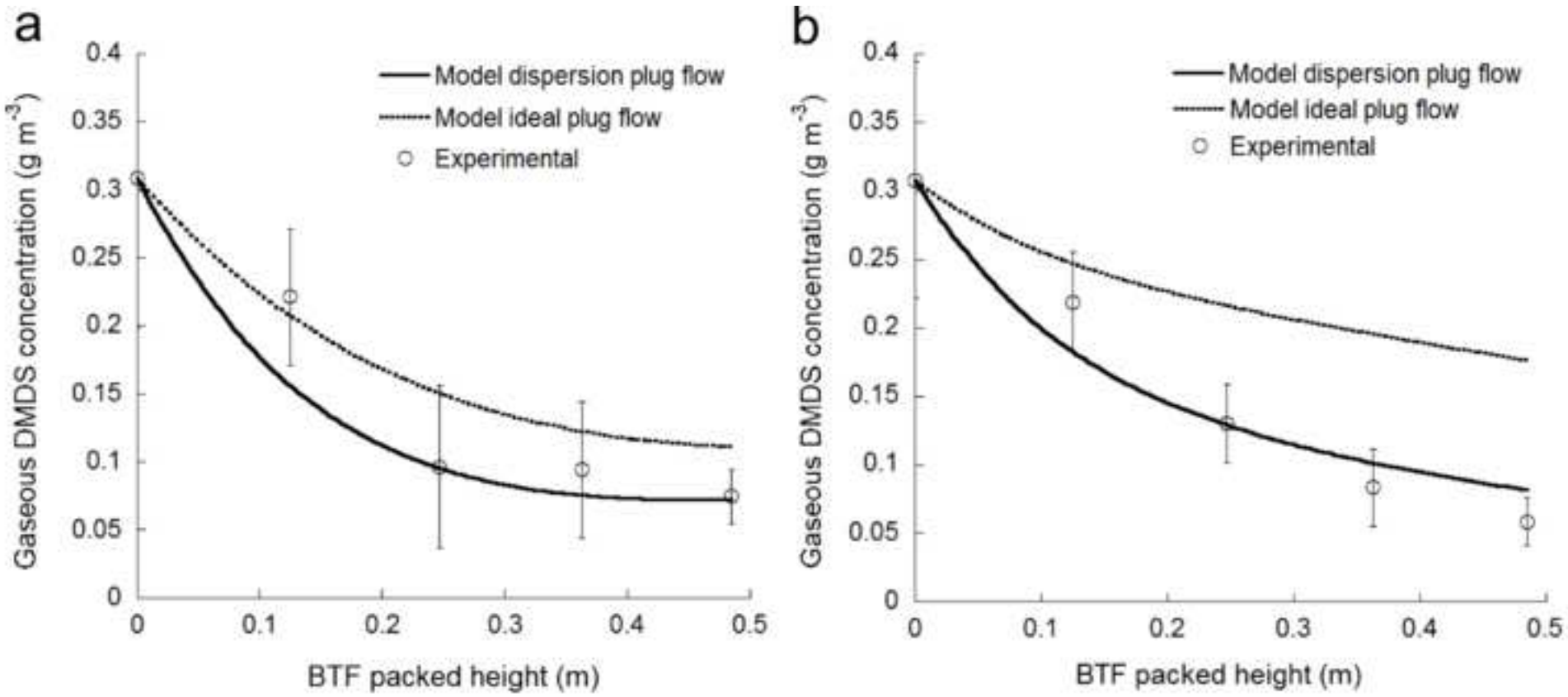

Figure 9
Click here to download high resolution image

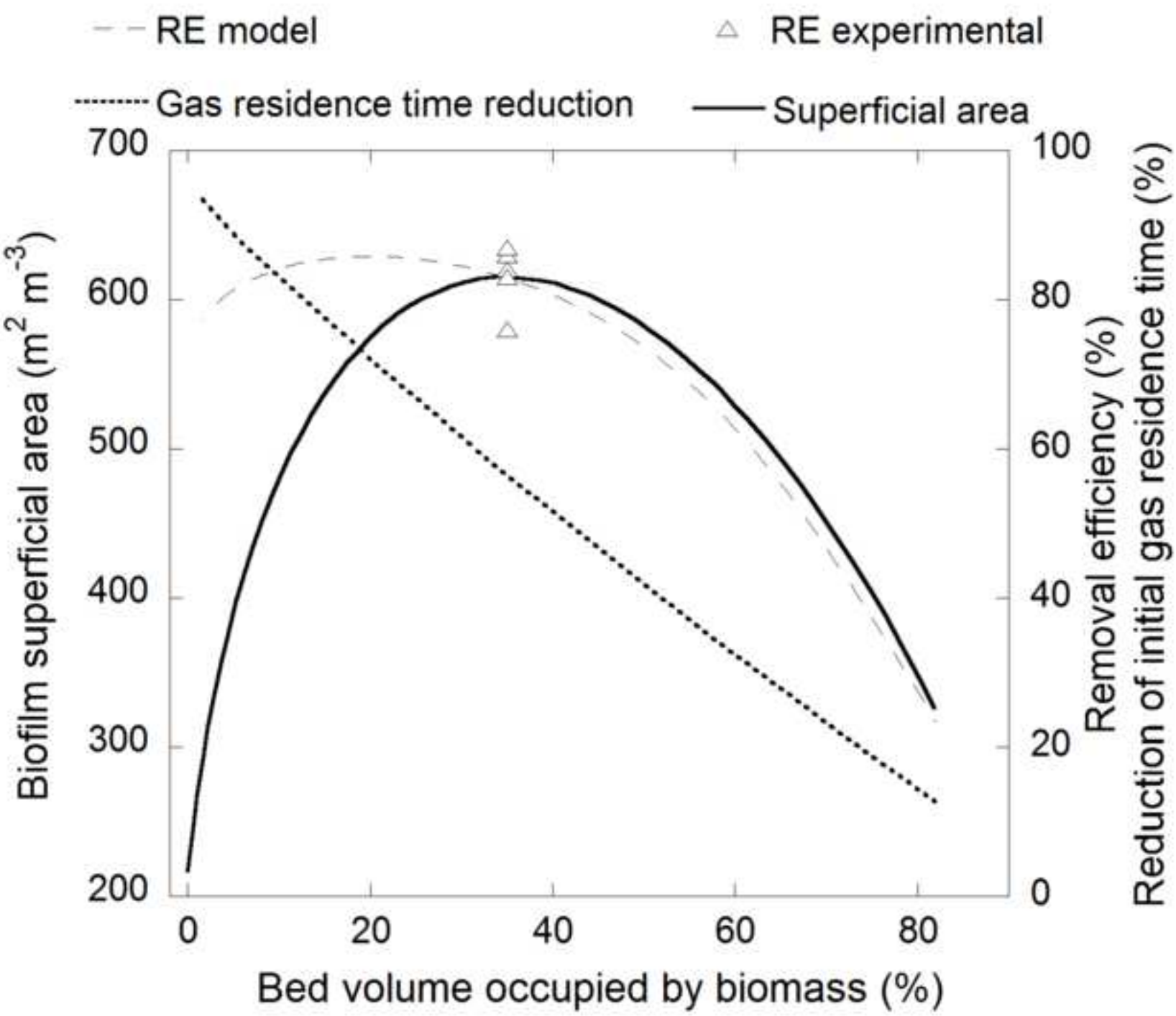

Supplementary Material

Click here to download Supplementary Material: Modeling_the_biomass_Supplement Information.docx